HHS Public Access

Author manuscript

Nat Neurosci. Author manuscript; available in PMC 2011 September 15.

Published in final edited form as:

Nat Neurosci. 2010 December ; 13(12): 1526–1533. doi:10.1038/nn.2682.

Tuning arousal with optogenetic modulation of locus coeruleus neurons

Matthew E. Carter[1,2], **Ofer Yizhar**[3], **Sachiko Chikahisa**[4,5], **Hieu Nguyen**[2], **Antoine Adamantidis**[2], **Seiji Nishino**[4], **Karl Deisseroth**[1,3], and **Luis de Lecea**[1,2]

[1]Neurosciences Program, Stanford University, Stanford, CA, 94305, USA

[2]Department of Psychiatry and Behavioral Sciences, Stanford University, Stanford, CA, 94305, USA

[3]Department of Bioengineering, Stanford University, Stanford, CA, 94305, USA

[4]Sleep & Circadian Neurobiology Laboratory, Stanford University, Stanford, CA, 94305, USA

[5]Department of Integrative Physiology, Institute of Health Biosciences, The University of Tokushima Graduate School, Tokushima 770-8503, Japan

Abstract

Neural activity in the noradrenergic locus coeruleus correlates with periods of wakefulness and arousal. However, whether tonic or phasic activity in these neurons is necessary or sufficient to induce behavioral state transitions and promote long-term arousal is unresolved. We used optogenetic tools in mice to demonstrate a frequency-dependent, causal relationship between locus coeruleus firing, cortical activity, sleep-to-wake transitions, and general locomotor arousal. Surprisingly, we also found that sustained, high-frequency stimulation of the locus coeruleus at frequencies 5 Hz and above caused reversible behavioral arrests. These results suggest that the locus coeruleus is finely tuned to regulate organismal arousal and that bursts of noradrenergic over-excitation cause behavioral attacks similar to those observed in neuropsychiatric disorders.

INTRODUCTION

The locus coeruleus is a noradrenergic brainstem structure that is thought to play a major role in promoting arousal[1–5]. Locus coeruleus neurons fire tonically from 1–3 Hz during awake states, decrease firing during NREM sleep, and are virtually silent during REM sleep[6–8]. The locus coeruleus also fires phasically in short bursts of 8–10 Hz during the presentation of salient stimuli which prolong wake states[7,9]. Importantly, alterations in

*Corresponding author: Luis de Lecea, Ph.D 1201 Welch Road MSLS Building room P107 Stanford, CA, 94305 Phone: 650-736-9039 Fax: 650-725-4913 llecea@stanford.edu.

AUTHOR CONTRIBUTIONS

M.E.C. and L.d.L. designed the study and wrote the manuscript. M.E.C. performed or assisted with all experiments. O.Y. performed and analyzed electrophysiology experiments, S.C. performed HPLC analysis, and H.N. analyzed immunohistochemical co-expression data. A.A. and L.d.L. provided expertise on optogenetic and polysomnographic recording techniques, as well as substantial feedback on the manuscript. S.N., K.D., and L.d.L. provided equipment, reagents, and critical feedback.

discharge rate precede changes in sleep-to-wake transitions[6,8,9]. However, whether this activity is causal or submissive remains unresolved, and the specific contributions of tonic versus phasic activity in modulating arousal states is unknown.

Experimentally determining a causal role for the locus coeruleus in promoting and maintaining arousal has remained elusive using traditional pharmacological and electrical techniques due to its small size, unique morphology, and proximity to neighboring brain structures[1,2]. Physical lesions of the locus coeruleus do not elicit consistent changes in cortical electroencephalography (EEG) or behavioral indices of arousal[10–12]. Genetic ablation of dopamine beta-hydroxylase, an enzyme necessary for norepinephrine synthesis, also does not disrupt sleep/wake states[13]. However, central injections of pharmacological antagonists for noradrenergic receptors[14] or agonists for inhibitory autoreceptors[15] cause substantial sedative effects. Alternatively, central administration of norepinephrine directly into the ventricles or forebrain promotes wakefulness[16,17]. Stimulation of locus coeruleus neurons using local microinjections of the cholinergic agonist bethanechol produces rapid activation of forebrain EEG in halothane-anesthetized rats[18]. Taken together, these results imply a role for the locus coeruleus in promoting arousal, but clearly new tools are necessary to selectively manipulate locus coeruleus discharge activity in freely moving, behaving animals at timescales relevant to natural sleep/wake events.

The recent development of optogenetic tools[19,20] provides a valuable opportunity to inhibit or stimulate activity in genetically-targeted neural populations with high spatial and temporal precision[21,22]. Therefore, to determine a conclusive, causal role for the locus coeruleus-norepinephrine system in promoting and maintaining wakefulness, we studied the effects of inhibiting locus coeruleus neurons with halorhodopsin (eNpHR)[23,24], a yellow-light sensitive chloride pump, or stimulating locus coeruleus neurons with channelrhodopsin-2 (ChR2)[25], a blue-light sensitive cation channel. We found that the locus coeruleus was necessary for maintenance of wake episodes but inhibition did not increase the duration of sleep episodes. Stimulation caused immediate sleep-to-wake transitions, extending the duration of wakefulness in a manner consistent with sleep deprivation. The probability of wakefulness during stimulation was finely tuned to both light pulse frequency and the duration of stimulation, indicating that the sleep/wake state of an animal is highly sensitive to activity in the locus coeruleus at a scale of single action potentials. Surprisingly, we also found that sustained (10–15 s) high frequency (>5 Hz) stimulation caused reversible behavioral arrests previously unknown to occur with locus coeruleus stimulation, suggesting a potential mechanism for the behavioral arrests present in some neuropsychiatric disorders.

RESULTS

Genetic targeting of locus coeruleus neurons

We genetically targeted locus coeruleus neurons by stereotaxically injecting a Cre-recombinase-dependent adeno-associated virus (rAAV)[26,27] into knockin mice selectively expressing Cre in tyrosine hydroxylase neurons[28] (**Supplementary Fig. 1**). We validated the specificity and efficiency of transgene expression by unilaterally injecting virus into the locus coeruleus region[29] and comparing viral eYFP expression with tyrosine hydroxylase immunofluorescence. eYFP fluorescence was detected throughout the entire locus coeruleus

but not in neighboring noradrenergic or dopaminergic regions (**Fig. 1a** and **Supplementary Fig. 2**). Out of 3463 tyrosine hydroxylase expressing neurons (n=4 mice), 98.1 +/– 1.9% co-expressed eYFP (**Fig. 1b**). Conversely, 97.9 +/– 2.9% of eYFP cells co-expressed tyrosine hydroxylase (**Fig. 1b**), demonstrating the specificity of viral targeting of the locus coeruleus.

To test the functional expression of optogenetic transgenes in locus coeruleus neurons, we recorded from eYFP-positive neurons in acute brainstem slices using the whole-cell patch clamp technique. In voltage-clamp mode, we found that eNpHR-transduced neurons exhibited rapid outward photocurrents upon illumination with yellow light (**Fig. 1c**), with a peak level of 435.5 +/– 44.2 pA and a steady-state level of 302.2 +/– 65.8 pA (mean +/– s.e.m.; n=5 cells). Alternatively, blue light photostimulation of ChR2-transduced neurons caused an inward steady state current of 321 +/– 50 pA (mean +/– s.e.m.; n=6 cells) (**Fig. 1d**). In current-clamp experiments, eNpHR-transduced neurons exhibited yellow light-evoked hyperpolarization, completely blocking endogenous spontaneous action potentials (**Fig. 1e**). In locus coeruleus neurons transduced with ChR2, 10 ms blue-light pulses caused action potentials from 1–30 Hz (**Fig. 1f**). The efficiency of ChR2-mediated spikes decreased with increasing frequency, with 100% efficiency at 20 Hz and below (**Fig. 1g**). Taken together, these *in vitro* results demonstrate that rAAV-mediated expression of eNpHR or ChR2 is sufficient to inhibit or stimulate action potentials in locus coeruleus neurons, respectively.

To modulate locus coeruleus neural activity *in vivo*, we bilaterally injected rAAV into each locus coeruleus region (**Supplementary Fig. 1c**), and implanted a bilateral cannula for subsequent light delivery. Electroencephalographic (EEG) and electromyographic (EMG) electrodes were placed in the skull and neck musculature, respectively, for sleep/wake analysis (**Supplementary Fig. 3**). Initial sleep recordings demonstrated that there was no difference in baseline sleep architecture between non-virally and virally transduced animals (n=4 animals per condition) (**Supplementary Fig. 4**).

To ensure the correct placement of cannulae and fiber optic cables, we applied long-term photostimulation (10 ms pulses at 3 Hz for 1 h) to the left locus coeruleus in ChR2-eYFP transduced mice or eYFP control mice (n=4 animals per condition) during the inactive (light) period and detected the presence of c-Fos, an indirect marker of neural activity (**Supplementary Fig. 5**). We found a significant increase in the number of tyrosine hydroxylase-positive cells that also expressed c-Fos between eYFP animals (17.2 +/–7.2%) and ChR2-eYFP animals (64.7 +/– 13.6%). Furthermore, c-Fos expression was found throughout the entire anteroposterior length of the locus coeruleus (**Supplementary Fig. 5c**), demonstrating the accuracy of our *in vivo* light delivery paradigm in stimulating the global population of locus coeruleus neurons.

To validate eNpHR-mediated inhibition of the locus coeruleus *in vivo*, we tested the effect of photoinhibition on norepinephrine content in prefrontal cortex, a region that only receives noradrenergic projections from the locus coeruleus. We delivered constant yellow light to the locus coeruleus in freely moving animals transduced with eNpHR-eYFP or eYFP (n=4 mice per condition) during the active (dark) period for 10 min while simultaneously using microdialysis to sample extracellular fluid in the prefrontal cortex. We found that 10 min of

continuous photoinhibition significantly decreased cortical norepinephrine concentration in eNpHR-eYFP but not eYFP control animals (**Supplementary Fig. 6**), demonstrating the utility of eNpHR-mediated photoinhibition *in vivo*.

Inhibition of the locus coeruleus reduces wakefulness

To determine the necessity of locus coeruleus neural activity in promoting wakefulness, we first tested the effect of long-term photoinhibition of the locus coeruleus (constant yellow light for 1 h) on sleep-wake architecture during both the inactive and active periods. We found no significant difference between eNpHR-eYFP and eYFP control animals (n=6 animals per condition) in the total duration of wake/sleep states during the inactive period (**Supplementary Fig. 7**). However, we found a significant decrease in the amount of wakefulness and significant increase in the amount of NREM sleep during the active period (**Fig. 2a**). During the active period, duration of individual wake episodes significantly decreased, but there was no significant change in the duration of NREM or REM episodes (**Fig. 2b**). We also found a significant increase in the number of wake-to-NREM transitions relative to baseline (no photoinhibition), but not an increase in any other sleep-state transitions (**Fig. 2c**), suggesting that the locus coeruleus is necessary for maintaining the normal duration of wake episodes.

To study the effects of locus coeruleus photoinhibition specifically during wakefulness, we restricted photoinhibition only to epochs when the animal was awake based on real-time, online EEG analysis. We found a significant reduction in wake episode duration in eNpHR-eYFP animals (n=6 animals) between baseline (no inhibition) and photoinhibition conditions (**Fig. 2d**), but no significant reduction of wake duration in photoinhibited eYFP control animals. Upon examination of the power spectrum of the cortical EEG towards the end of wake episodes (80–120 s from the onset of wakefulness in wake episodes lasting at least 120 s), we found no difference in the relative slow wave activity (SWA, 0.5–4 Hz), a hallmark of sleep pressure, between eNpHR-eYFP and control animals in baseline (no inhibition) conditions (**Fig. 2e**, top). However, during photoinhibition, there was a statistically significant increase in SWA between eYFP and eNpHR-eYFP mice ($P<0.05$, Student's t-test between transduced mice), demonstrating an increase in the propensity of eNpHR-eYFP animals to enter NREM sleep (**Fig. 2e**, bottom). Taken together, these results suggest that the locus coeruleus is necessary for maintaining normal durations of wakefulness during the active period.

Stimulation of the locus coeruleus causes wake transitions

We next investigated a causal role for locus coeruleus neurons in promoting wakefulness by testing the effect of photostimulation on sleep-to-wake transitions during the inactive period. We initially tested the effect of 5 Hz blue light stimulation for 5 s (10 ms pulses) during NREM sleep, always beginning stimulation trials 15 s after the onset of NREM sleep. Stimulation at these parameters reliably produced immediate sleep-to-wake transitions within 5 s of the onset of stimulation in ChR2-eYFP animals but not eYFP control animals (n=6 animals per condition) (**Fig. 3a** and **Supplementary Movie 1**). In ChR2-eYFP animals, photostimulation produced immediate changes in the cortical EEG with a significant decrease in SWA ($P<0.001$ using a two-tailed Student's t-test between pre-

stimulation and stimulation conditions) (**Fig. 3b**). To precisely determine the effects of various photostimulation frequencies and durations on sleep-to-wake transitions, we stimulated eYFP and ChR2-eYFP animals at frequencies of 1–10 Hz and durations of 1–10 s (all light pulses 10 ms in duration), measuring the probability of a NREM-to-wake transition within 10 s of the onset of stimulation. We found that the probability of a NREM-to-wake transition increased with stimulation frequency and duration in ChR2-eYFP animals but not control animals (**Fig. 3c**).

We then repeated the experiments above but studied the effect of photostimulation on REM sleep-to-wake transitions. Photostimulation at 5 Hz for 5 s (10 ms pulses) in ChR2-eYFP animals also caused immediate REM sleep-to-wake transitions (**Fig. 3d**), with immediate changes in the cortical EEG and a significant decrease in the theta activity (4–9 Hz) that characterizes REM sleep ($P<0.001$ using a two-tailed Student's t-test between pre-stimulation and stimulation conditions) (**Fig. 3e**). As in NREM sleep, increasing the frequency and duration of stimulation increased the probability of sleep-to-wake transitions (**Fig. 3f**).

The relationship between the duration and frequency of stimulation necessary to cause a 100% probability of sleep-to-wake transitions was linear and inversely proportional during both NREM (**Fig. 3c** and **Supplementary Fig. 8a**) and REM sleep (**Fig. 3f** and **Supplementary Fig. 8b**). We also explored the number of photostimulation pulses required for a sleep-to-wake transition. As the frequency of stimulation increased, the number of pulses required for a 100% probability of awakening decreased for both NREM (**Supplementary Fig. 8c**) and REM (**Supplementary Fig. 8d**). Interestingly, as the duration of stimulation increased, the number of pulses required for a 100% probability of awakening increased for both NREM (**Supplementary Fig. 8e**) and REM sleep (**Supplementary Fig. 8f**).

To determine if locus coeruleus-mediated sleep-to-wake transitions depend on norepinephrine release, we repeated photostimulation experiments (10 ms pulses at 5 Hz for 5 s) in ChR2-eYFP animals (n=4) 30 min after administration of the adrenergic α2 receptor agonist clonidine or α1 receptor antagonist prazosin, compounds that both result in suppressing NE transmission. In saline-injected ChR2 animals, photostimulation always caused sleep-to-wake transitions (probability=1.00). We found that administration of both clonidine and prazosin reduced the probability of NREM and REM sleep-to-wake transitions in a dose-dependent manner (**Supplementary Fig. 9**). These results demonstrate that locus coeruleus-mediated sleep-to-wake transitions depend, at least in part, on normal NE transmission.

Long-term stimulation of locus coeruleus neurons

To determine the effects of long-term stimulation on arousal, we photostimulated locus coeruleus neurons for one hour during the inactive period and measured changes in sleep/wake duration and general locomotor activity. Previous physiological recordings of the locus coeruleus demonstrate that neurons fire tonically from 1–3 Hz during wakefulness[6-8], and also phasically in short bursts (500 ms) of 8-10 Hz during the presentation of salient

stimuli which prolong wake states[7,9]. Therefore, we decided to study the effects of long-term stimulation using both tonic and phasic stimulation paradigms to see if there were differential effects on arousal. Tonic stimulation consisted of constant 10 ms light pulses at 3 Hz while phasic stimulation consisted of 10 ms pulses at 10 Hz for 500 ms (5 light pulses) every 20 s.

We found that both tonic and phasic stimulation paradigms increased the total amount of wakefulness and decreased the total amount of NREM sleep in ChR2-eYFP compared with eYFP animals (n=5 animals per condition) (**Fig. 4a,b**). The reduction in sleep caused by photostimulation of locus coeruleus neurons at tonic and phasic frequencies can be considered a model of sleep deprivation, as the following hour (without photostimulation) showed hallmarks of sleep pressure including a rebound of NREM sleep and a significant increase in slow wave activity (SWA) in the cortical EEG ($P<0.05$, Student's t-test between baseline and 1 h post-stimulation conditions) (**Fig. 4c,d**). Interestingly, we found that tonic versus phasic stimulation of locus coeruleus neurons caused differential effects on locomotor activity: tonic stimulation caused a significant increase in locomotor activity over the hour of stimulation (**Fig. 4e**) while phasic stimulation caused a significant decrease (**Fig. 4f**). Finally, we wondered if tonic or phasic stimulation would increase the total duration of wakefulness over longer time periods of 5 hours. We found that, unlike 1 h of stimulation, tonic stimulation at 3 Hz for 5 h did not result in a significant difference in the total duration of wakefulness or NREM sleep states between ChR2-eYFP compared with eYFP animals (n=5 animals per condition) (**Fig. 4g**). Alternatively, phasic stimulation for 5 h resulted in a significant increase in the total amount of wakefulness and decease in the total amount of NREM sleep (**Fig. 4h**).

Taken together, these results indicate that long-term, tonic stimulation of locus coeruleus neurons over 1 h causes an increase in wakefulness and general locomotor activity, but the effects of stimulation decline over a 5 h period. Long-term, phasic stimulation of locus coeruleus neurons causes an increase in wakefulness over both 1 and 5 h periods but with a decrease in locomotor activity.

High-frequency stimulation of locus coeruleus neurons

Surprisingly, we found that sustained photostimulation of the locus coeruleus at frequencies 5 Hz and above caused reversible behavioral arrests (**Fig. 5a** and **Supplementary Movie 2**). At the onset of stimulation, mice began a 5–20 s period of increased locomotor behavior leading to eventual immobility. After the laser diode was switched off, mice remained immobile with their eyes open for 15–20 s and then fully recovered movement. During the behavioral arrest, mice were unresponsive to tail and toe pinch. Only stimulation frequencies of 5 Hz and above produced behavioral arrests, with a 100% probability at 15 Hz and above (**Fig. 5b**). These arrests were caused by both unilateral and bilateral photostimulation; unilateral stimulation did not produce any obvious unilateral motor effects such as turning or direction-bias. Increasing stimulation frequencies caused decreases in the latency to arrest (time from light onset to immobility), however, the stimulation frequency that caused the arrest had no effect on the duration of arrest (time from light offset to recovery of movement) (**Fig. 5c**).

We hypothesized that high-frequency stimulation of the locus coeruleus caused behavioral arrests due to seizure or a severe cardiovascular response. However, we detected no signs of spike discharge in the cortical EEG characteristic of seizure activity (**Fig. 5d**). Instead, theta rhythm activity was prominent in the EEG across multiple animals (n=6 mice) throughout most of the behavioral arrest episodes (**Fig. 5e**). We also found no difference in heart rate or systolic blood pressure between baseline conditions and during behavioral arrests (n=4 mice) (**Supplementary Fig. 10**).

We also investigated the effect of high-frequency stimulation on NE release. Using *in vivo* microdialysis to sample extracellular fluid from the prefrontal cortex, we found that extracellular NE concentration substantially decreased during 10 min of continuous stimulation at 10 Hz in ChR2-eYFP compared with eYFP animals (n=4 animals per condition) (**Fig. 5f**). However, there was no statistical difference between the percentage decrease in cortical NE elicited by 10 Hz stimulation in ChR2-eYFP animals (n=4 animals), which caused behavioral arrests, and constant photoinhibition in eNpHR-eYFP animals (n=4 animals; **Supplementary Fig. 6**), which did not cause behavioral arrests ($P>0.05$, two-way ANOVA between stimulation condition and transgene expression). To determine the effects of increasing extracellular NE concentration on behavioral arrests, we stimulated ChR2-eYFP animals (n=4) 30 minutes after administration of the NE reuptake inhibitors atomoxitine or reboxitine. We found a dose dependent increase in the latency to arrest and decrease in the duration of arrest (**Fig. 5g**). Taken together, these results demonstrate that sustained, high frequency stimulation of locus coeruleus neurons causes a depletion of NE stores and that increasing NE concentration using reuptake inhibitors attenuates the arrests.

DISCUSSION

Tuning arousal with modulation of locus coeruleus neurons

This study demonstrates that neural activity in the locus coeruleus is both necessary for maintaining normal durations of wakefulness as well as sufficient to promote immediate sleep-to-wake transitions, long-term wakefulness, and an increase in locomotor arousal. Taken together, these results suggest that the locus coeruleus is finely-tuned to influence wakefulness, with even subtle differences in stimulation frequency and duration causing different effects on arousal and sleep-to-wake transitions (**Supplementary Fig. 11**). Anatomically, the locus coeruleus receives many afferent projections[2,30] and is well-positioned to receive input from hypothalamic and brainstem circuits that sense salient environmental and homeostatic stimuli[31-33], as well as information from higher-cognitive circuits in the prefrontal cortex[34]. In turn, the locus coeruleus projects extensively to virtually all brain regions with the exception of the striatum[2]. Therefore, the anatomical connections of the locus coeruleus, combined with our *in vivo* behavioral results, suggest that the locus coeruleus integrates information from lower and higher neural circuits and is finely-tuned to affect downstream nuclei and modulate behavior.

Although our *in vitro* recordings from locus coeruleus neurons in acute brainstem slices demonstrate the efficiency of eNpHR-mediated photoinhibition and the reliability of 10 ms blue-light pulses in causing single spikes, we cannot be certain that these tools modulate neural activity as precisely *in vivo*. We found that inhibition of the locus coeruleus using

yellow light significantly decreased cortical norepinephrine concentration (**Supplementary Fig. 6**) and that stimulation using blue light significantly increased expression of the immediate early gene c-Fos throughout the entire anteroposterior length of the locus coeruleus (**Supplementary Fig. 5**). However, we cannot be certain of the efficiency of these tools in inhibiting or stimulating single action potentials in awake, behaving animals. At the same time, our results clearly show differential effects that vary linearly based on the frequency and duration of stimulation (**Supplementary Fig. 8**). Therefore, we conclude that the locus coeruleus is finely-tuned to influence behavior depending on different stimulation parameters.

Previous studies in which the locus coeruleus was pharmacologically lesioned[10-12] or NE transmission was genetically ablated[13] found no significant differences in durations of sleep and wakefulness. In contrast, we found a significant reduction in wake episode duration during 1 h of eNpHR-mediated inhibition of the locus coeruleus during the active period (**Fig. 2**). A major advantage of eNpHR to traditional pharmacological or genetic loss-of-function methods is the ability to silence neural activity at specifically defined temporal windows with minimal disturbance to the animal. Perhaps permanently ablating locus coeruleus neurons or norepinephrine synthesis causes the brain to adapt using other wake-promoting systems[4], as has been reported for other brain circuits, such as those involved in food intake[35,36]. Furthermore, our rAAV-mediated genetic targeting of the locus coeruleus was able to bilaterally transduce >98% of locus coeruleus neurons, a higher percentage than previous studies using radiofrequency pulses[10], saporin[12], or DSP-4[37]. Therefore, our loss-of-function approach achieved not only acute temporal specificity but also efficient genetic targeting of the locus coeruleus, which may explain our novel results.

eNpHR-mediated inhibition of the locus coeruleus caused a decrease in the duration of wakefulness and an increase in slow-wave activity in the EEG power spectra at the end of wake episodes (**Fig. 2**). However, inhibition did not prevent sleep-to-wake transitions, nor increase the duration of sleep episodes. In contrast to inhibition, we found that stimulation of the locus coeruleus caused immediate sleep-to-wake transitions (**Fig. 3**). Therefore, we conclude that the locus coeruleus is sufficient to promote sleep-to-wake transitions, but other nuclei must contribute to sleep-to-wake transitions in a way that is statistically redundant with locus coeruleus activity. Other known arousal-promoting nuclei include the histaminergic tuberomammilary nucleus (TMN)[38], the serotoninergic dorsal raphe nuclei[39], the cholinergic pedunculopontine nucleus and lateral tegmental nucleus[40,41], as well as multiple cell-types in the basal forebrain[42]. Perhaps the locus coeruleus plays a more prominent, necessary role in promoting wakefulness when the animal is already awake, but is sufficient to promote arousal in a way that is redundant with other arousal systems when the animal is asleep.

Importantly, we show differential effects on arousal using naturally occurring tonic versus phasic stimulation paradigms (**Fig. 4**). Long-term tonic stimulation over 1 h caused an increase in the duration of wakefulness, as well as an increase in locomotor activity; however, this paradigm was not sufficient to increase the duration of wakefulness over 5 h of stimulation. In contrast, long-term phasic stimulation caused an increase in the duration of wakefulness over 1 h and 5 h, but a decrease in locomotor activity. Previous studies in

which locus coeruleus activity was recorded in rats and primates demonstrate that tonic locus coeruleus activity is correlated with wakefulness, firing at 3 Hz during active wakefulness, 1-2 Hz during quiet wakefulness, <1 Hz during NREM sleep, and not firing during REM sleep[6-8]. Phasic locus coeruleus activity correlates with salient environmental stimuli[7,9] and has been proposed to underly mechanisms of attention and behavioral/cognitive adaptation to changing environmental circumstances[1,2,5,43-45]. Therefore, perhaps tonic stimulation at low frequencies (3 Hz) specifically causes an increase in arousal, while phasic frequencies may also cause changes in cortical networks and synaptic plasticity that alters cognition or attention, resulting in loss of exploratory/locomotor behavior. Furthermore, presenting phasic stimulation without environmental stimuli that cause endogenous phasic activation of the locus coeruleus may confound cortical networks and result in a lack of locomotion.

Tonic versus phasic frequencies are also thought to differentially affect different categories of noradrenergic receptors[1,2,44]: norepinephrine has the highest affinity for the α2-receptors, which are found on both pre- and post-synaptic terminals and cause hyperpolarizing effects. Norepinephrine has lower affinities for the α1- and β-receptors, which are primarily post-synaptic. Therefore, it is thought that low, tonic release of norepinephrine may preferentially activate α2-receptors, while high-frequency, phasic release of NE may preferentially activate α1- and β-receptors. Perhaps tonic stimulation of locus coeruleus neurons promotes wakefulness during 1 h, but is insufficient to increase arousal at longer time periods due to steady activation of α2-receptors, leading to self-inhibition of the locus coeruleus and inhibition of downstream targets. Alternatively, phasic stimulation of locus coeruleus neurons may cause long-term activation of α1- and β-receptors, allowing animals to consistently maintain wakefulness over longer time periods.

The locus coeruleus can cause behavioral arrests

A surprising and novel finding of our study is that sustained high frequency (>5 Hz) stimulation of the locus coeruleus causes reversible behavioral arrests (**Fig. 5**). We hypothesized that these arrests were caused by seizure or a severe cardiovascular response, but found no signs of spike discharge in the cortical EEG characteristic of seizure activity or statistically significant differences in heart rate or blood pressure (**Fig. 5e** and **Supplementary Fig. 10**).

Interestingly, using microdialysis to sample extracellular fluid from the cortex, we found that high-frequency stimulation of the locus coeruleus caused a *decrease* in cortical norepinephrine concentration (**Fig. 5f**), suggesting that high-frequency, non-physiological levels of stimulation depleted norepinephrine from locus coeruleus terminals. Unfortunately, microdialysis has a temporal resolution of several minutes, preventing detection of norepinephrine discharge rates over the 10-15 s of high frequency stimulation necessary to cause behavioral arrests. Voltammetry techniques have better temporal resolutions but are not good at distinguishing between norepinephrine and other catecholamines. We hypothesize that high-frequency stimulation of the locus coeruleus causes first a rapid increase of extracellular norepinephrine concentration over several seconds, followed by the decrease observed by our microdialysis data. The decrease in norepinephrine content could

be due to a breakdown of cortical norepinephrine in the synapse and the inability of locus coeruleus terminals to replenish norepinephrine while still firing at >5 Hz stimulation. At the offset of blue light stimulation, the locus coeruleus terminals could replenish norepinephrine stores, allowing the animal to recover. Indeed, increasing extracellular norepinephrine by preventing reuptake attenuated the arrests (**Fig. 5f**).

However, behavioral arrests cannot be caused solely by a decrease in brain norepinephrine content, as eNpHR-mediated inhibition produced statistically similar decreases in cortical norepinephrine concentrations without producing arrests (**Supplementary Fig. 6**). Futhermore, previous studies in which locus coeruleus activity was ablated did not produce behavioral arrests[10-12]. The inability of photoinhibition to cause arrests may be due to the synergistic effects of other neuromodulatory systems. For example, it has been shown that serotonin cell activity (and presumably serotonin release) is greatly decreased in cataplexy[46] and REM sleep[47]. Thus, inhibiting the locus coeruleus during tonic activity of raphe neurons may allow muscle tone to be maintained by serotonin. It has also been shown with microdialysis that GABAergic and glycinergic release is increased during muscle tone suppression[48], causing active inhibition in motoneurons. Excessive firing of norepinephrine neurons may trigger the activity of post-synaptic inhibitory neurons in the brainstem eliciting a behavioral arrest.

Behavioral arrests may be caused by non-endogenous norepinephrine release onto noradrenergic receptors. As discussed above, α1- and β-receptors may be preferentially activated by phasic versus tonic frequencies. Therefore, the high-frequency stimulation that elicits locus coeruleus-mediated behavioral arrests may cause dramatic, non-endogenous activation of α1 and β-receptors, followed by a relative loss of extracellular norepinephrine as indicated by our microdialysis results (**Fig. 5f**). This rapid release followed by depletion is an unexplored phenomenon on post-synaptic terminals, and future *in vitro* research using slice preparations is necessary to understand the consequences of a rapid efflux of norepinephrine release at postsynaptic sites.

The locus coeruleus-mediated behavioral arrests described here may cause the motor arrests associated with symptoms of some neuropsychiatric disorders with no known etiology. Interestingly, locus coeruleus-mediated behavioral arrests are not inconsistent with a mouse model of cataplexy as recently defined by the International Working Group on Rodent Models of Narcolepsy[49]. This condition is generally defined by an abrupt episode of nuchal atonia lasting at least 10 seconds with EEG characteristic of theta activity and at least 40 seconds of wakefulness preceding the episode. Our characterization of locus coeruleus-mediated behavioral arrests fit these criteria (**Fig. 5**). However, locus coeruleus-mediated arrests are likely to be analogous rather than homologous to murine cataplexy, as the locus coeruleus has been previously shown to be silent preceding cataplectic attacks[50] rather than exhibiting the high frequencies reported here. Nevertheless, based on our results, the consensus definition of cataplexy may need to be revised, and it will be important for future studies to consider the role of the locus coeruleus in mediating the symptoms of other neuropsychiatric diseases.

Supplementary Material

Refer to Web version on PubMed Central for supplementary material.

ACKNOWLEDGEMENTS

We thank members of the de Lecea lab for helpful advice and feedback. Thanks to Jennifer Shieh for assistance with confocal images, Anne Hilgendorff for assistance with mouse cardiovascular measurements, and Simon Xie for access to custom-built SmartCages. M.E.C. received financial support from an NSF Graduate Research Fellowship and the NIH National Research Service Award (F31MH83439). O.Y. is supported by a European Molecular Biology Organization long-term postdoctoral fellowship. S.C. is supported by the Excellent Young Researcher Overseas Visit Program (21-8162) of JSPS. A.A. is supported by fellowships from the Fonds National de la Recherche Scientifique ("Charge de Recherche"), NIH (K99), and NARSAD. S.N. is supported by NIH grant R01MH072525. K.D. is supported by NSF, National Institute of Mental Health, National Institute on Drug Abuse, and the McKnight, Coulter, Snyder, Albert Yu and Mary Bechmann, and Keck foundations. L.d.L. is supported by the NIH (MH83702, MH87592, DA21880) and NARSAD.

ONLINE METHODS

Animals

Tyrosine hydroxylase (TH)::IRES-Cre knockin mice[28] (EM:00254) were obtained from the European Mouse Mutant Archive and mated with c57Bl/6 wild-type mice. This study used only male heterozygous mice, aged 8-10 weeks at the start of experimental procedures and no more than 18 weeks at the end of experimental procedures. Mice were housed in individual plexiglass recording chambers residing in custom-designed stainless steel cabinets at constant temperature (22 +/– 1° C), humidity (40-60%), and circadian cycle (12 h light/dark cycle, starting at 9:00 A.M.). Food and water were available *ad libitum*. All experiments were performed in accordance with the guidelines described in the National Institutes of Health *Guide for the Care and Use of Laboratory Animals*.

Virus preparation

Cre-inducible recombinant AAV vectors carrying optogenetic transgenes were serotyped with AAV5 coat proteins and packaged by the viral vector core at the University of North Carolina. The final viral concentration was 2×10^{12} genome copies (gc)/mL. Aliquots of virus were stored at –80 °C prior to stereotaxic injection

Surgery

At the start of surgical procedures, mice were anesthetized with ketamine/xylazine anesthesia (80 and 16 mg/kg, i.p., respectively) and placed on a small animal stereotaxic frame (David Kopf Instruments). Recombinant AAV5 carrying Ef1α::eNpHR-eYFP, Ef1α::ChR2-eYFP, or control Ef1α::eYFP was unilaterally or bilaterally injected adjacent to the locus coeruleus [anteroposterior (AP), 5.45 mm; mediolateral (ML), +/– 1.28 mm; dorsoventral (DV) 3.65 mm][29] through an internal cannula (Plastics One) at a rate of 0.1 μl/min for 10 min (1 μl total volume) (**Supplementary Fig. 1**). Animals receiving unilateral injections were used for initial viral expression experiments (**Fig. 1**) and no further surgical procedures took place. Animals receiving bilateral injections were used for all other experiments and received additional surgical implants, described below.

Following viral injection, animals received surgical implantation of a 26G bilateral cannula (Plastics One) with 2 mm between individual cannulae and 3 mm shaft length (**Supplementary Fig. 3**). The cannula was placed above the locus coeruleus region (AP, 5.45 mm; ML, +/– 1.0 mm; DV, 3.0 mm) and affixed to the skull with C&B Metabond (Parkell) and dental acrylic.

Animals used for sleep recordings were also implanted with a custom-made EEG/EMG implant placed anterior to the cannula (**Supplementary Fig. 3**). EEG signals were recorded from electrodes placed on the frontal (AP, –2 mm; ML, +/– 2.5 mm) and temporal (AP, 3 mm; ML, +/– 2.5 mm) cortices. EMG signals were recorded from two electrodes inserted in the neck musculature to record postural tone.

After surgical procedures, animals were allowed to recover in individual housing for at least two weeks. Animals used for sleep recordings were then acclimated to a flexible EEG/EMG connection cable for an additional 7 d within individual recording chambers. Each cable was flexible so that mice could freely move about their cages. Fiber optic cables were implanted at least 2 days prior to experiments and ran alongside the EEG/EMG connection cables (**Supplementary Fig. 3**).

Electrophysiology

Acute brainstem coronal slices (250 μm) were collected on a vibratome and prepared as previously described[21]. Transduced locus coeruleus neurons were identified via eYFP fluorescence. Whole-cell recordings were conducted using a Multiclamp 700B and signals were digitized at 10 kHz.

Polysomnographic recording and analysis

All sleep recordings took place between 12:00–18:00 (light onset at 9:00) except for photoinhibition experiments that took place in the active (dark) period, which took place between 21:00–24:00 (light offset at 21:00). EEG and EMG signals derived from the surgically implanted electrodes were amplified (Grass Instruments) and digitized at 256 Hz using sleep recording software (Vital Recorder, Kissei Comtec America). The signals were digitally filtered and spectrally analyzed by fast Fourier transformation, and polysomnographic recordings were scored using sleep analysis software (SleepSign for Animal, Kissei Comtec America). All scoring was performed manually based on the visual signature of the EEG and EMG waveforms, as well as the power spectra of 5 s epochs.

We defined wakefulness as desynchronized low-amplitude EEG and heightened tonic EMG activity with phasic bursts. We defined NREM sleep as synchronized, high-amplitude, low-frequency (0.5–4 Hz) EEG and highly reduced EMG activity compared with wakefulness with no phasic bursts. We defined REM sleep as having a pronounced theta rhythm (4–9 Hz) and a flat EMG. All sleep-scoring was done by an investigator (M.E.C.) blind to the viral transgene delivered to the animal and to baseline vs. stimulation/inhibition conditions.

Photostimulation and Photoinhibition

All photostimulation experiments except for c-Fos expression analysis (**Supplementary Fig. 5**) were conducted bilaterally. Fiber optic cables (2 m long, 200 μm diameter; ThorLabs) were placed inside the implanted cannulae 2 h prior to stimulation/inhibition experiments. Mice were allowed at least 2 days to acclimate prior to experimental sessions. For photostimulation experiments, light pulse trains (10 ms pulses of various frequency and duration, as indicated in the text) were programmed using a waveform generator (33220A Waveform Generator, Agilent Technologies) that provided simultaneous input into two blue-light lasers (473 nm, 20 mW light intensity; LaserGlo). For acute photostimulation experiments, each stimulation epoch was applied 15 s after the occurrence of a stable NREM or REM sleep event as detected by real-time online EEG/EMG analysis. For photoinhibition experiments, light delivery was provided by a yellow-light laser (593 nm; LaserGlo) split into two fiber optic cables.

Cardiovascular measurements

We measured heart rate and blood pressure in mice during photostimulation experiments using a tail cuff attached to a MK-2000ST Blood Pressure Monitor for Mice (Muromachi). Mice were acclimated to a mouse holder and blood pressure was measured at a starting pressure of 50 mm Hg.

Microdialysis and high pressure liquid chromatography (HPLC)

Animals used for microdialysis experiments (**Fig. 5** and **Supplementary Fig. 6**) were surgically implanted with a microdialysis cannula (EICOM) with 1 mm shaft length. The cannulae was placed in prefrontal cortex (AP, 1.5 mm; ML, 0.5 mm; DV, 1 mm) and affixed to the skull with C&B Metabond and dental acrylic.

During experiments, a microdialysis probe (EICOM) with 1 mm membrane length was placed within the guide cannula and the mouse was allowed a 30 min acclimation period before perfusion. During collection, we continuously perfused fresh artificial cerebrospinal fluid (aCSF: 147 mM NaCl, 2.8 mM KCl, 1.2 mM $CaCl_2$, 1.2 mM $MgCl_2$ in H_20) at a rate of 1 μL per minute for a total of 10 minutes for each sample. Dialysates were collected into chilled 0.5 ml tubes containing 10 μl aCSF with 0.02 M acetic acid. Each experimental session lasted 70 min: 3 × 10 min for baseline measurements, 1 × 10 min for measurements during photostimulation with 10 Hz blue light (**Fig. 5**) or inhibition with yellow light (**Supplementary Fig. 6**), and 3 × 10 min recovery measurements.

Norepinephrine levels in the dialysate were determined by HPLC with electrochemical detection. Microdialysis samples (10 μL dialysate and 10 μl aCSF with 0.02 M acetic acid) were mixed with 20 μl 0.1 M acetic acid containing 0.27 mM EDTA. Samples were injected using an autoinjector (Bio-Rad, Hercule, CA). The HPLC mobile phase (0.1 M Sodium phosphate buffer, 0.13 mM EDTA, 2.3 mM 1-octanesulfonic acid, 7% MeOH, pH 6.0) was pumped through a chromatography column (SC-5ODS, EICOM) and a 20 μl sample loop at a flow rate of 0.23 ml/min. A graphite electrode set (WE-3G, EICOM) at a potential of 460 mV was used for electrochemical detection and quantified with a PowerChrom analysis

system (ADInstruments) using external norepinephrine standards (Sigma, St. Louis, MO). Norepinephrine concentrations were calculated by comparing the HPLC peak of norepinephrine in each sample with the peak area of known concentrations of the standards analyzed on the same day.

Histology

After completion of experiments, mice were anesthetized with ketamine/xylazine anesthesia (80 and 16 mg/kg, i.p., respectively) and perfused transcardially with 1X PBS, pH 7.4, followed by 4% paraformaldehyde in PBS. The brains were extracted, allowed to postfix overnight in the same fixative at 4 °C, and cryoprotected in 30% sucrose dissolved in 1X PBS for an additional 24 h at 4 °C. Each brain was sectioned at 30 μm on a cryostat (Leica Microsystems) and collected in cold PBS.

For co-localization experiments (**Fig. 1a** and **Supplementary Fig. 2**), brain sections from eYFP transduced mice were washed in PBS with 0.3% Triton X-100 (PBST) for 10 min at room temperature. Sections were then incubated in a blocking solution composed of PBST with 4% bovine serum albumin and 2% normal horse serum for 1 h at room temperature. For primary antibody exposure, sections were incubated in chicken anti-tyrosine hydroxylase (1:2000, Aves Labs, #TH) in block solution at 4 °C for approximately 16 h. Following 3 × 10 min washes in PBST, sections were incubated in Alexa Fluor 568 goat anti-chicken IgG secondary antibody (1:500, Molecular Probes, #A-11041) in block solution for 1 h at room temperature. Sections were washed 3 × 1X PBS, mounted onto SuperFrost Plus glass slides (VWR, #48311-703), and coverslipped with VECTASHIELD with DAPI Mounting Media (Vector Laboratories, #H-1200). Quantification of colocalization was performed on adjacent sections from approximately bregma –5.20 to –5.80 (exactly 21 sections per mouse).

For c-Fos experiments (**Supplementary Fig. 5a**), brain sections from eYFP and ChR2-eYFP transduced mice were washed in PBST and incubated in a 3% hydrogen peroxide solution for 30 min at room temperature. After a brief wash in PBST, sections were incubated in block solution for 1 h at room temperature. Sections were incubated in rabbit anti-c-Fos (1:5000, Calbiochem, #PC05) in block solution at 4 °C for approximately 16 h. Following 3 × 10 min washes in PBST, sections were incubated in biotinylated goat anti-rabbit IgG secondary antibody (1:500, Vector Laboratories, #BA-1000) for 1 h at room temperature. Next, the sections were washed 3 × 10 min in PBST and incubated in an avidin-biotin ABC peroxidase solution (Vector Laboratories, #PK-6100) for 30 min at room temperature. Finally, the sections were washed 3 × 10 min in 1X PBS and stained using 3-3'diaminobenzidine-4 HCl (DAB) and nickel solution (Vector Laboratories, SK-4100) to produce a black staining product.

After this initial round of staining for the presence of c-Fos, sections were submitted to a second round of staining for tyrosine hydroxylase. After a brief wash in PBST, sections were incubated in chicken anti-tyrosine hydroxylase (1:2000, Aves Labs, #TH) in block solution at 4 °C for approximately 16 h. Following 3 × 10 min washes in PBST, sections were incubated in biotinylated goat anti-chicken IgG secondary antibody (1:500, Vector Laboratories, #BA-9010) for 1 h at room temperature. Next, the sections were washed 3 ×

10 min in PBST and incubated in an avidin-biotin ABC peroxidase solution (Vector Laboratories, #PK-6100) for 30 min at room temperature. Finally, the sections were washed 3 × 10 min in 1X PBS and stained using DAB alone to produce a brown staining product. After 3 × 5 min washes in 1X PBS, processed sections were mounted onto slides and coverslipped using Permaslip (Alban Scientific). As in viral expression experiments, quantification of colocalization of c-Fos immunofluorescence (black) and tyrosine hydroxylase immunofluorescence (brown) was performed on adjacent sections from approximately bregma –5.20 to –5.80 (exactly 21 sections total per mouse). Tyrosine hydroxylase-positive cells were scored for the presence of c-Fos by an investigator (M.E.C.) blind to the side of stimulation and identity of the virally-transduced mouse (eYFP or ChR2-eYFP).

Microscopy

Non-confocal images were collected on a Carl Zeiss fluorescent microscope either using fluorescent reflected light (**Fig.1a**, top row, and **Supplementary Fig. 2**) or brightfield transmitted light (**Supplementary Fig. 5a**). Confocal images (**Fig. 1a**, bottom rows) were collected on a Zeiss LSM 510 Meta confocal microscope. Digital images were minimally processed using Adobe Photoshop CS3 (Adobe Systems) to enhance brightness and contrast for optimal representation of the data. All digital images were processed in the same way between experimental conditions to avoid artificial manipulation between different datasets.

Statistics

All data were analyzed using Prism 5.0 (GraphPad Software) as described in the text. Data were exported into Adobe Illustrator CS3 (Adobe Systems) for preparation of figures.

REFERENCES

1. Aston-Jones G, Cohen JD. An integrative theory of locus coeruleus-norepinephrine function: adaptive gain and optimal performance. Annu. Rev. Neurosci. 2005; 28:403–450. [PubMed: 16022602]
2. Berridge CW, Waterhouse BD. The locus coeruleus-noradrenergic system: modulation of behavioral state and state-dependent cognitive processes. Brain Res. Rev. 2003; 42:33–84. [PubMed: 12668290]
3. Foote SL, Bloom FE, Aston-Jones G. Nucleus locus ceruleus: new evidence of anatomical and physiological specificity. Physiol. Rev. 1983; 63:844–914. [PubMed: 6308694]
4. Saper CB, Scammell TE, Lu J. Hypothalamic regulation of sleep and circadian rhyhms. Nature. 2005; 437:1257–1263. [PubMed: 16251950]
5. Sara SJ. The locus coeruleus and noradrenergic modulation of cognition. Nature Rev. Neurosci. 2009; 10:211–223. [PubMed: 19190638]
6. Aston-Jones G, Bloom FE. Activity of norepinephrine-containing locus coeruleus neurons in behaving rats anticipates fluctuations in the sleep-waking cycle. J. Neurosci. 1981; 1:876–886. [PubMed: 7346592]
7. Aston-Jones G, Bloom FE. Norepinephrine-containing locus coeruleus neurons in behaving rats exhibit pronounced responses to non-noxious environmental stimuli. J. Neurosci. 1981; 1:887–900. [PubMed: 7346593]
8. Hobson JA, McCarley RW, Wyzinski PW. Sleep cycle oscillation: reciprocal discharge by two brainstem neuronal groups. Science. 1975; 189:55–58. [PubMed: 1094539]

9. Foote SL, Aston-Jones G, Bloom FE. Impulse activity of locus coeruleus neurons in awake rats and monkeys is a function of sensory stimulation and arousal. Proc. Natl. Acad. Sci. 1980; 77:3033–3037. [PubMed: 6771765]
10. Jones BE, Harper ST, Halaris AE. Effects of locus coeruleus lesions upon cerebral monoamine content, sleep-wakefulness states and the response to amphetamine in the cat. Brain Res. 1977; 124:473–496. [PubMed: 192414]
11. Lidbrink P. The effect of lesions of ascending noradrenaline pathways on sleep and waking in the rat. Brain Res. 1974; 74:19–40. [PubMed: 4152613]
12. Blanco-Centurion C, Gerashchenko D, Shiromani PJ. Effects of saporin-induced lesions of three arousal populations on daily levels of sleep and wake. J. Neurosci. 2007; 27:14041–14048. [PubMed: 18094243]
13. Hunsley MS, Palmiter RD. Norepinephrine-deficient mice exhibit normal sleep-wake states but have shorter sleep latency after mild stress and low doses of amphetamine. Sleep. 2003; 26:521–526. [PubMed: 12938804]
14. Berridge CW, Espana RA. Synergistic sedative effects of noradrenergic alpha(1)- and beta-receptor blockade on forebrain electroencephalographic and behavioral indices. Neuroscience. 2000; 99:495–505. [PubMed: 11029541]
15. De Sarro GB, Ascioti C, Froio F, Libri V, Nistico F. Evidence that locus coeruleus is the site where clonidine and drugs acting at alpha 1- and alpha 2-adrenoceptors affect sleep and arousal mechanisms. Br. J. Pharmacol. 1987; 90:675–685. [PubMed: 2884006]
16. Flicker C, Geyer MA. The hippocampus as a possible site of action for increased locomotion during intracerebral infusions of norepinephrine. Behav. Neural Biol. 1982; 34:421–426. [PubMed: 7126090]
17. Segal DS, Mandell AJ. Behavioral activation of rats during intraventricular infusion of norepinephrine. Proc. Natl. Acad. Sci. U.S.A. 1970; 66:289–293. [PubMed: 5271164]
18. Berridge CW, Foote SL. Effects of locus coeruleus activation on electroencephalographic activity in neocortex and hippocampus. J. Neurosci. 1991; 11:3135–3145. [PubMed: 1682425]
19. Gradinaru V, et al. Targeting and readout strategies for fast optical neural control in vitro and in vivo. J. Neurosci. 2007; 27:14231–14238. [PubMed: 18160630]
20. Zhang F, Aravanis AM, Adamantidis A, de Lecea L, Deisseroth K. Circuit-breakers: optical technologies for probing neural signals and systems. Nature Rev. Neurosci. 2007; 8:577–581. [PubMed: 17643087]
21. Adamantidis A, Zhang F, Aravanis AM, Deisseroth K, de Lecea L. Neural substrates of awakening probed with optogenetic control of hypocretin neurons. Nature. 2007; 450:420–424. [PubMed: 17943086]
22. Carter ME, Adamantidis A, Ohtsu H, Deisseroth K, de Lecea L. Sleep homeostasis modulates hypocretin-mediated sleep-to-wake transitions. J. Neurosci. 2009; 29:10939–10949. [PubMed: 19726652]
23. Gradinaru V, Thompson KR, Deisseroth K. eNpHR: a Natronomonas halorhodopsin enhanced for optogenetic applications. Brain Cell Biol. 2008; 36:129–139. [PubMed: 18677566]
24. Zhang F, et al. Multimodal fast optical interrogation of neural circuitry. Nature. 2007; 446:633–639. [PubMed: 17410168]
25. Boyden ES, Zhang F, Bamberg E, Nagel G, Deisseroth K. Millisecond-timescale, genetically targeted optical control of neural activity. Nature Neurosci. 2005; 8:1263–1268. [PubMed: 16116447]
26. Sohal VS, Zhang F, Yizhar O, Deisseroth K. Parvalbumin neurons and gamma rhythms enhance cortical circuit performance. Nature. 2009; 459:698–702. [PubMed: 19396159]
27. Tsai HC, et al. Phasic firing in dopaminergic neurons is sufficient for behavioral conditioning. Science. 2009; 324:1080–1084. [PubMed: 19389999]
28. Lindeberg J, et al. Transgenic expression of Cre recombinase from the tyrosine hydroxylase locus. Genesis. 2004; 40:67–73. [PubMed: 15452869]
29. Paxinos, G.; Franklin, K. The Mouse Brain in Stereotaxic Coordinates. ed. 2. Academic Press; New York: p. 2001

30. Shipley MT, et al. Dendrites of locus coeruleus neurons extend preferentially into two pericoerulear zones. J. Comp. Neurol. 1996; 365:56–68. [PubMed: 8821441]
31. Bourgin P, et al. Hypocretin-1 modulates rapid eye movement sleep through activation of locus coeruleus neurons. J. Neurosci. 2000; 20:7760–7765. [PubMed: 11027239]
32. Valentino R, et al. Corticotropin-releasing factor innervation of the locus coeruleus region: distribution of fibers and sources of input. Neuroscience. 1992; 48:689–705. [PubMed: 1376457]
33. van Bockstaele EJ, et al. Anatomic basis for differential regulation of the rostrolateral peri-locus coeruleus region by limbic afferents. Biol Psychiatry. 1999; 46:1352–1363. [PubMed: 10578450]
34. Jodo E, Chiang C, Aston-Jones G. Potent excitatory influence of prefrontal cortex activity on noradrenergic locus coreuleus neurons. Neuroscience. 1998; 83:63–79. [PubMed: 9466399]
35. Luquet S, Perez FA, Hnasko TS, Palmiter RD. NPY/AgRP neurons are essential for feeding in adult mice but can be ablated in neonates. Science. 2005; 310:683–685. [PubMed: 16254186]
36. Wu Q, Boyle MP, Palmiter RD. Loss of GABAergic signaling by AgRP neurons to the parabrachial nucleus leads to starvation. Cell. 2009; 137:1225–1234. [PubMed: 19563755]
37. Szot P, et al. A comprehensive analysis of the effect of DSP4 on the locus coeruleus noradrenergic system in the rat. Neuropharmacology. 2010; 166:279–291.
38. Parmentier R, et al. Anatomical, physiological, and pharmacological characteristics of histidine decarboxylase knock-out mice: evidence for the role of brain histamine in behavioral and sleep-wake control. J Neurosci. 2002; 22:7695–7711. [PubMed: 12196593]
39. McGinty DJ, Harper RM. Dorsal raphe neurons: depression of firing during sleep in cats. Brain Res. 1976; 101:569–575. [PubMed: 1244990]
40. Steriade M. Acetycholine systems and rhythmic activities during the waking—sleep cycle. Prog. Brain Res. 2004; 145:179–196. [PubMed: 14650916]
41. Boucetta S, Jones BE. Activity profiles of cholinergic and intermingled GABAergic and putative glutamatergic neurons in the pontomesencelphalic tegmentum of urethane-anesthetized rats. J. Neurosci. 2009; 29:4664–4674. [PubMed: 19357291]
42. Hassani OK, Lee MG, Henny P, Jones BE. Discharge profiles of identified GABAergic in comparison to cholinergic and putative glutamatergic basal forebrain neurons across the sleep-wake cycle. J. Neurosci. 2009; 29:11828–11840. [PubMed: 19776269]
43. Arnsten A. Stress signaling pathways that impair prefrontal cortex structure and function. Nat. Rev. Neurosci. 2009; 10:410–422. [PubMed: 19455173]
44. Ramos B, Arnsten A. Adrenergic pharmacology and cognition: Focus on the prefrontal cortex. Pharmacol. Ther. 2006; 113:523–536. [PubMed: 17303246]
45. Bouret S, Sara SJ. Network reset: a simplified overarching theory of locus coeruleus noradrenaline function. Trends Neurosci. 2005; 28:574–582. [PubMed: 16165227]
46. Wu MF, et al. Activity of dorsal raphe cells across the sleep-waking cycle and during cataplexy in narcoleptic dogs. J. Physiol. 2004; 554:202–215. [PubMed: 14678502]
47. Lai YY, Kodama T, Siegel JM. Changes in monoamine release in the ventral horn and hypoglossal nucleus linked to pontine inhibition of muscle tone: an *in vivo* microdialysis study. J. Neurosci. 2001; 21:7384–7391. [PubMed: 11549748]
48. Kodama T, Lai YY, Siegel JM. Changes in inhibitory amino acid release linked to pontine-induced atonia: an *in vivo* microdialysis study. J. Neurosci. 2003; 23:1548–1554. [PubMed: 12598643]
49. Scammell TE, et al. A consensus definition of cataplexy in mouse models of narcolepsy. Sleep. 2009; 32:111–116. [PubMed: 19189786]
50. Wu MF, et al. Locus coeruleus neurons: cessation of activity during cataplexy. Neuroscience. 1999; 91:1389–1399. [PubMed: 10391445]

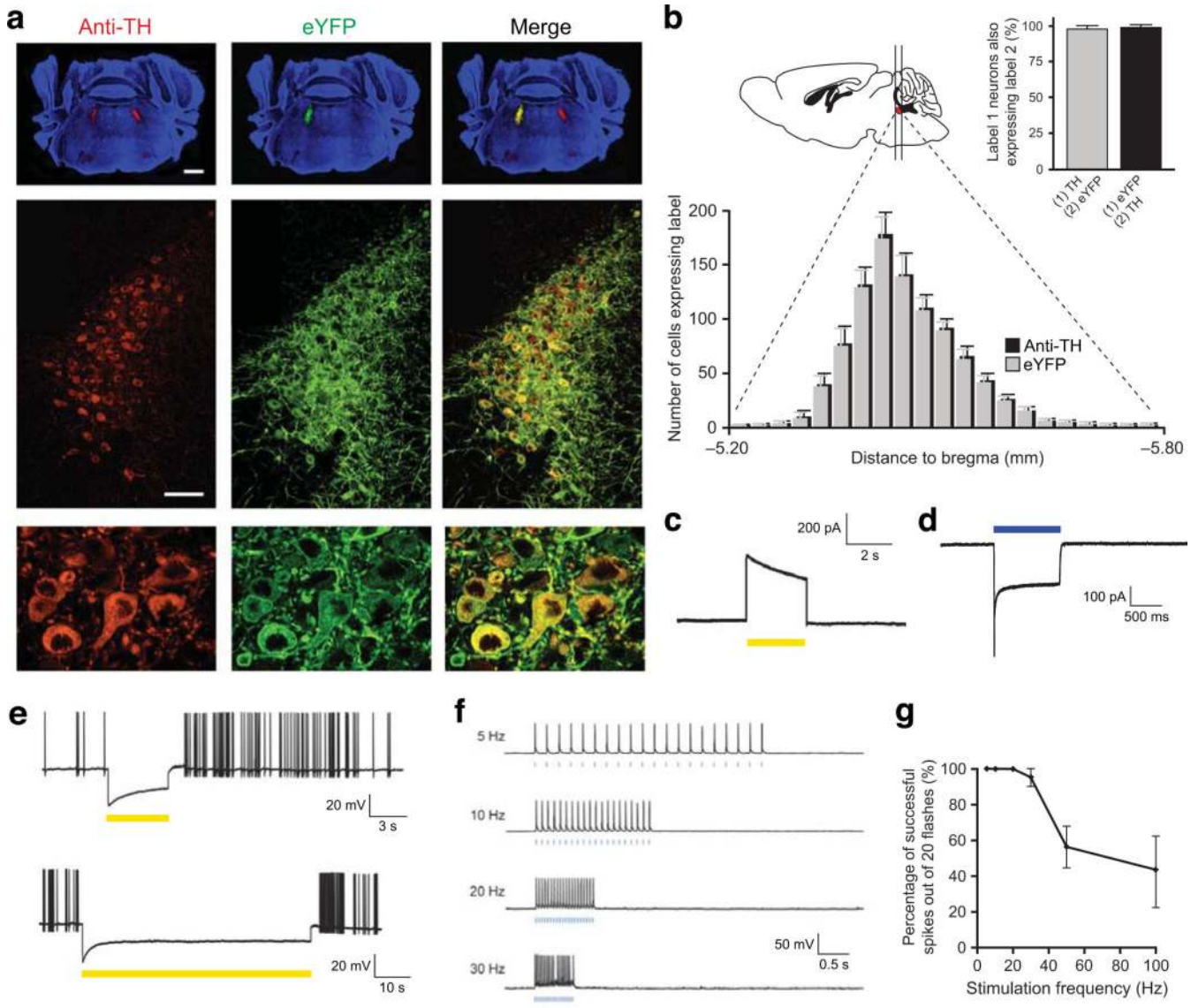

Figure 1.

Specific and efficient functional expression of optogenetic transgenes in locus coeruleus neurons. **(a)** Representative photomicrographs depicting tyrosine hydroxylase (TH) immunoreactivity (left column, red), viral eYFP expression (center column, green), and merged images (right column) from an animal unilaterally injected with EF1α::eYFP rAAV virus into the left locus coeruleus region. Top row shows global expression in a coronal section counterstained with DAPI (scale bar, 100μm); middle row shows expression within the full locus coeruleus (scale bar, 25 μm); bottom row shows individual neurons (scale bar, 5 μm). **(b)** Quantification of co-expression of eYFP and TH immunofluorescence from EF1α::eYFP transduced mice (n=4) in 30 μm brain sections from the rostral-to-caudal ends of the locus coeruleus (anteroposterior, –5.20 to –5.80). Cell counts are represented as mean +/– s.d. Inset represents the statistics of the total co-expression **(c)** Voltage clamp recording of a neuron expressing eNpHR-eYFP in brainstem slice showing outward current in response to yellow light. **(d)** Voltage clamp recording of a neuron expressing ChR2-eYFP in

brainstem slice showing inward current in response to blue light. **(e)** Action potential trains recorded under current clamp conditions from a neuron expressing eNpHR-eYFP in brainstem slice for 5 s (top) or 1 min (bottom). **(f)** Blue-light pulse trains (10 ms per pulse) evoked action potential trains in neurons expressing ChR2-eYFP at various frequencies. **(g)** Efficiency of action potential trains evoked by blue light pulses in ChR2-eYFP expressing neurons. Data represent mean probability +/– s.e.m. from n=6 neurons.

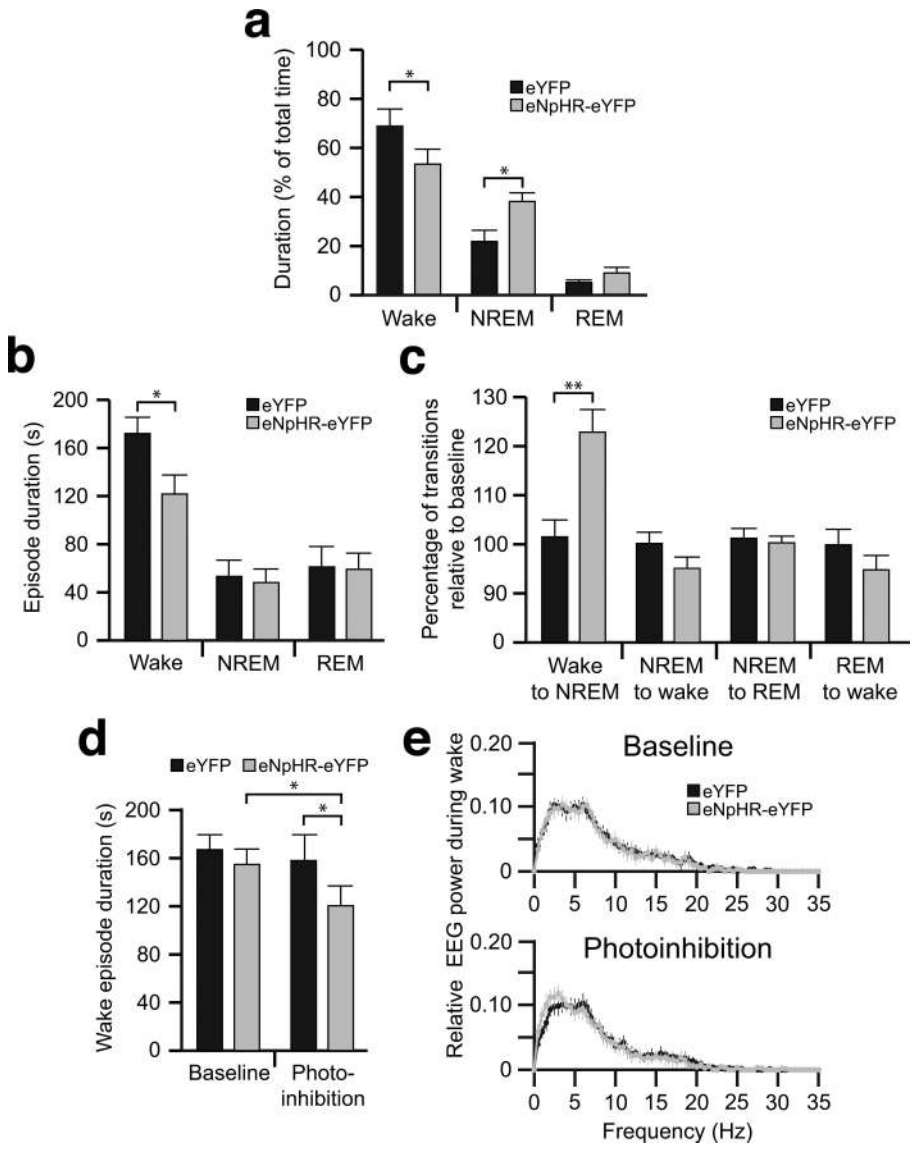

Figure 2.

Photoinhibition of locus coeruleus neurons causes a reduction in the duration of wakefulness. **(a)** The percentage of time spent in wake, NREM, and REM sleep during 1 h photoinhibition in the active (dark) period. Data represent the mean +/– s.e.m. of 6 separate 1 h sessions, n=6 animals throughout. *P<0.05, two-tailed Student's t-test between transduced animals. **(b)** The duration of individual wake, NREM, and REM episodes during 1 h photoinhibition during the active period. *P<0.05, two-tailed Student's t-test between transduced animals. **(c)** The percentage of sleep state transitions relative to baseline levels during 1 h photoinhibition during the active period. **P<0.001, two-tailed Student's t-test between transduced animals. **(d)** The duration of individual wake episodes in baseline versus photoinhibition conditions (20 episodes per mouse, n=6 mice). *P<0.05, two-way ANOVA between stimulation condition and viral transduction followed by Tukey posthoc test. **(e)** Relative EEG power of wakefulness between 80-120 s after wake-onset in baseline (top) and

photoinhibition (bottom) conditions. Data represent the mean +/– s.e.m. relative power of 0.5 Hz binned frequencies (20 episodes per mouse, n=6 mice).

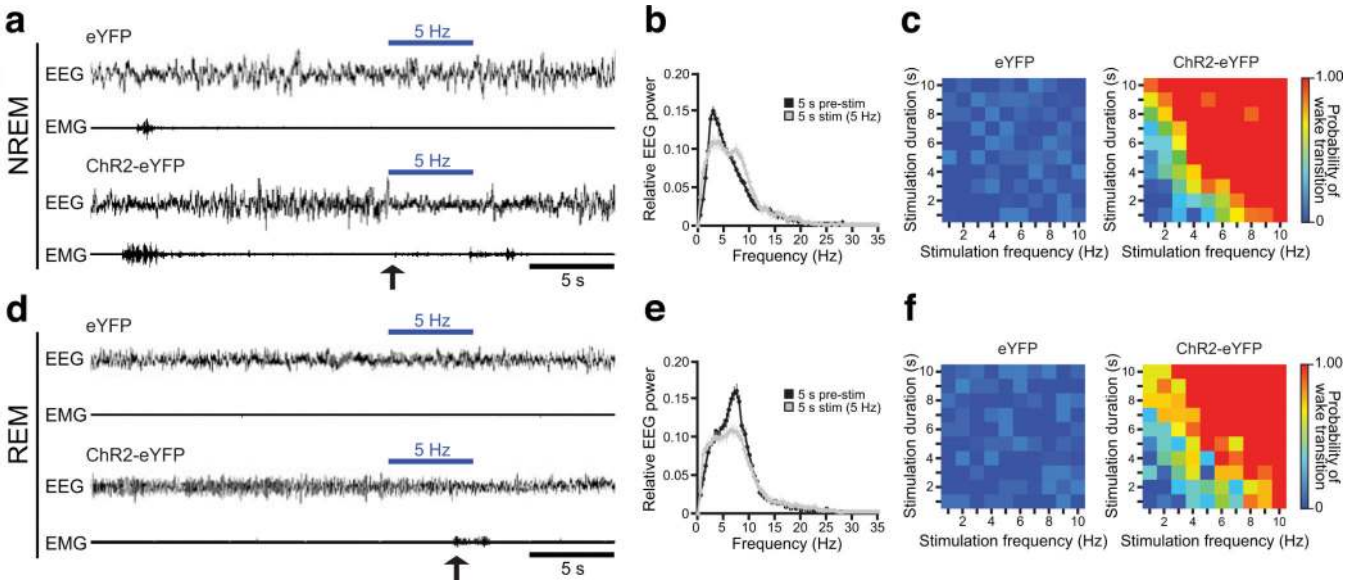

Figure 3.

Photostimulation of locus coeruleus neurons causes immediate sleep-to-wake transitions. **(a,d)** Representative traces of EEG/EMG recordings showing an immediate (a) NREM or (d) REM sleep-to-wake transition following acute photostimulation (10 ms pulses at 5 Hz for 5 s) of locus coeruleus neurons during the inactive period in a mouse transduced with ChR2-eYFP (bottom) but no awakening in a mouse transduced with eYFP alone (top). Arrow indicates onset of sleep-to-wake transition. **(b,e)** Cortical EEG traces from ChR2-eYFP mice 5 s prior to the onset of stimulation (black) and 5 s during stimulation (grey). Quantification is based on the average of (b) 15 or (e) 8 stimulations per mouse, n=6 mice. **(c,f)** Heat maps showing the effects of photostimulation on (c) NREM or (f) REM sleep-to-wake transitions in eYFP (n=6) or ChR2-eYFP (n=6) transduced animals. Each square represents the mean probability of a sleep-to-wake transition within 10 s of the onset of stimulation. Data analysis is based on the average of (c) 15 or (f) 8 stimulations per condition per mouse.

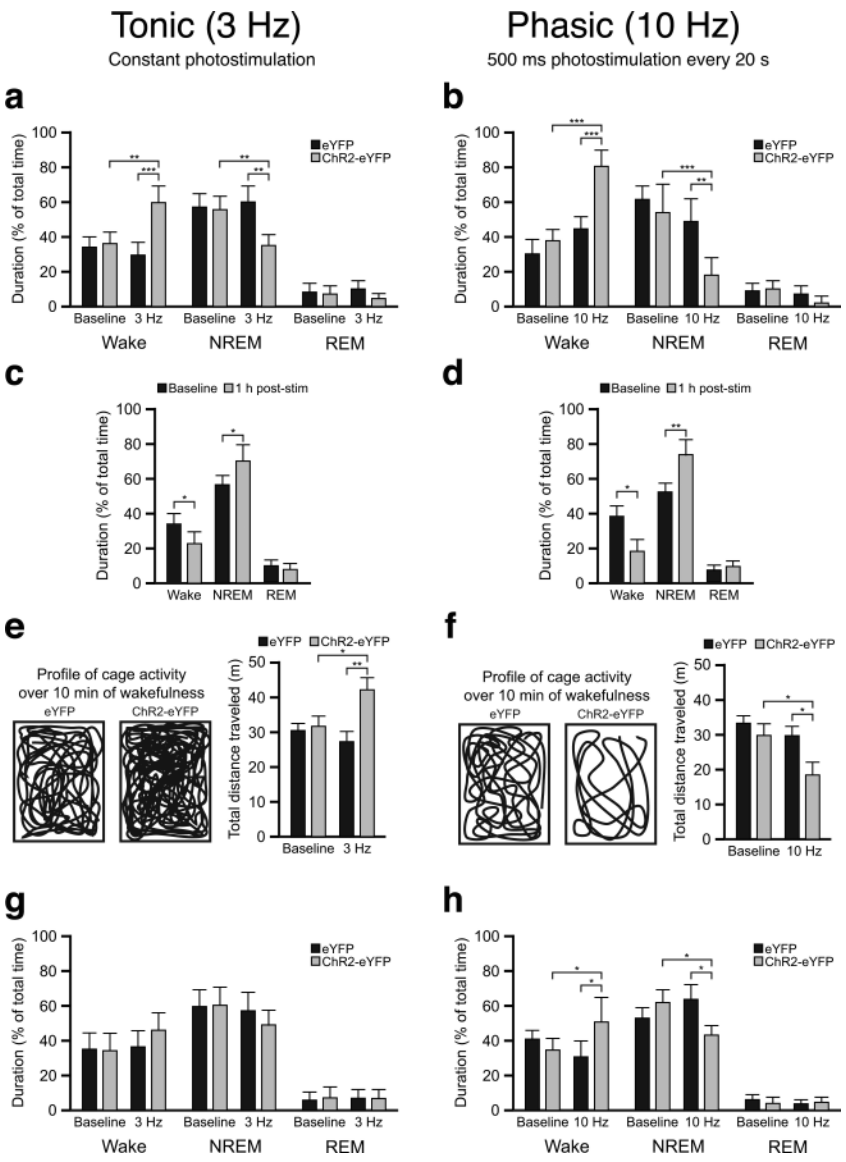

Figure 4.

Long-term tonic versus phasic stimulation of the locus coeruleus causes differential promotion of arousal. Tonic (consistent 10 ms pulses at 3 Hz) and phasic (10 ms pulses at 10 Hz for 500 ms occurring every 20 s) stimulation protocols are consistent throughout. **(a,b)** The effect of (a) tonic or (b) phasic photostimulation for 1 h on sleep architecture in ChR2-eYFP (n=5) or eYFP (n=5) transduced mice. Data represent the mean +/- s.e.m. percentage time over four trials spent in wake, NREM sleep, or REM sleep in baseline conditions or during photostimulation. $^{**}P<0.001$, $^{***}P<0.0001$, two-way ANOVA between stimulation condition and viral transduction, followed by Tukey posthoc test. **(c,d)** Sleep recordings in the hour following (c) tonic or (d) phasic photostimulation. $^{*}P<0.05$, $^{**}P<0.001$, Student's t-test. **(e,f)** Representative trace of locomotor activity in an eYFP and ChR2-eYFP transduced mouse during (e) tonic or (f) phasic photostimulation for 1 h during a 10 min wake period. Quantification at right shows the mean +/– s.e.m. distance traveled by eYFP (n=5) or ChR2-eYFP (n=5) transduced animals over the 1 h of photostimulation after 5

sessions of stimulation per mouse. *P<0.05, **P<0.001, two-way ANOVA between stimulation condition and viral transduction, followed by Tukey posthoc test. **(g,h)** The effect of (g) tonic or (h) phasic photostimulation for 5 h on sleep architecture in ChR2-eYFP (n=5) or eYFP (n=5) transduced mice. *P<0.05, two-way ANOVA between stimulation condition and viral transduction, followed by Tukey posthoc test.

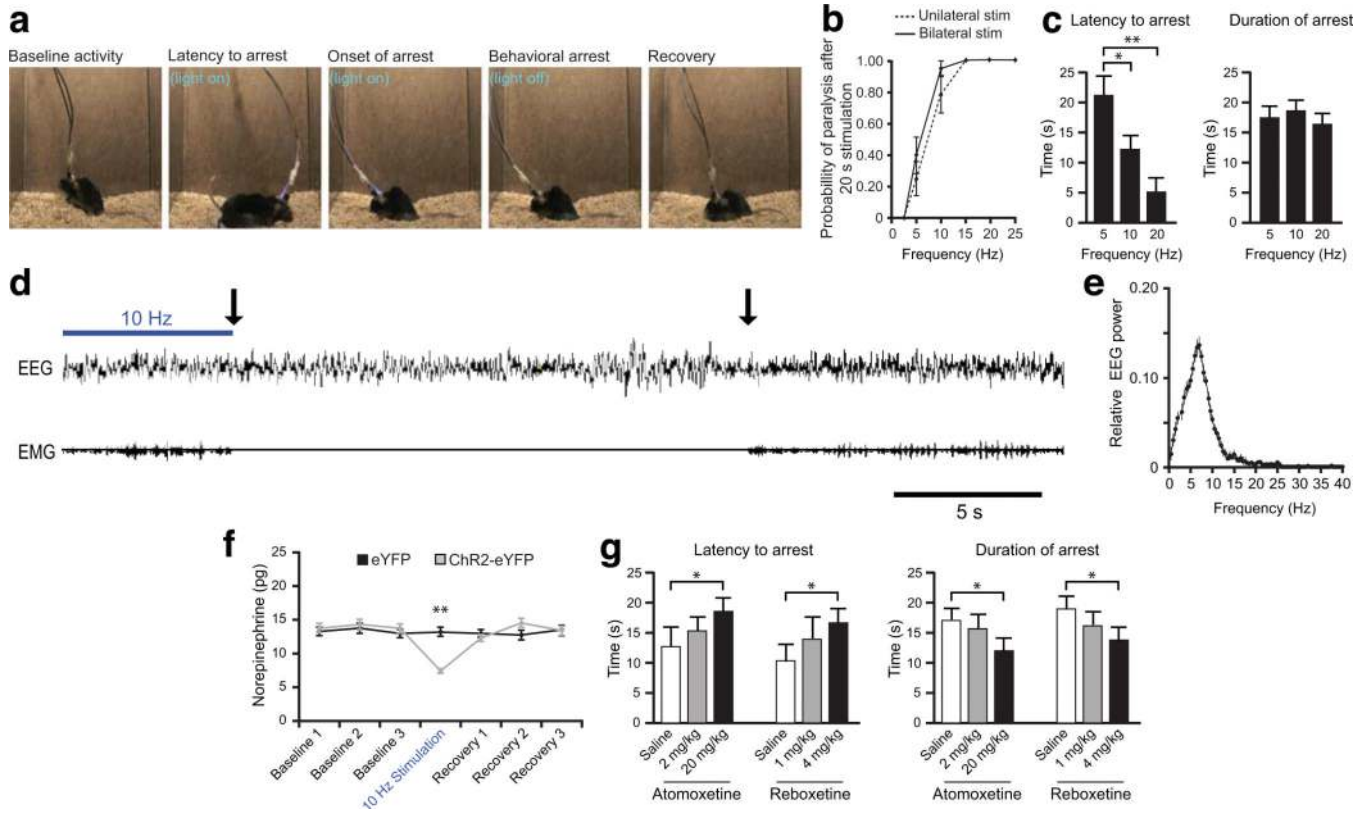

Figure 5.

High-frequency photostimulation of the locus coeruleus causes reversible behavioral arrests. **(a)** Sequence of events in a behavioral arrest. **(b)** Probability of behavioral arrests depends on photostimulation frequency. Data represent mean +/– s.e.m. of ChR2-eYFP transduced animals (n=4 animals, 10 trials per frequency per mouse). **(c)** The duration of latencies to arrest (time from light onset until behavioral arrest) and durations of arrest (time between the onset and offset of behavioral arrest) in ChR2-eYFP stimulated animals. Data represent the mean +/– s.e.m. of 20 trials per animal, n=8 animals. **P*<0.05, ***P*<0.001 between frequencies, ANOVA followed by Tukey posthoc test. **(d)** Representative EEG/EMG trace of a behavioral arrest following 10 Hz photostimulation. Arrows represent the onset and offset of immobility. **(e)** Relative EEG power of the first 10 s of behavioral arrests across multiple animals. Data represent the mean +/– s.e.m. relative power of 0.5 Hz binned frequencies (20 episodes per mouse, n=6 mice). **(f)** Measurement of extracellular norepinephrine content in prefrontal cortex during 10 Hz stimulation. Data represent the mean +/– s.e.m. of 3 trials per animal, n=4 animals. ***P*<0.001, two-way ANOVA between timepoint and virally-transduced animal followed by Bonferroni post-hoc test. **(g)** The duration of latencies to arrest and durations of arrest in ChR2-eYFP stimulated animals upon administration of the norepinephrine reuptake inhibitors atomoxetine or reboxetine. Data represent the mean +/– s.e.m. of 10 trials per animal, n=4 animals. Increased darkness of bars represents increasing pharmacological dose. **P*<0.05, Student's t-test between saline and drug-injected animals.